Characterization of the Brillouin grating spectra in a polarization-maintaining fiber

Yongkang Dong,[1,2] Liang Chen,[1] and Xiaoyi Bao[1,3]

[1]*Fiber Optics Group, Department of Physics, University of Ottawa, Ottawa, K1N 6N5, Canada*
[2]*aldendong@gmail.com*
[3]*xbao@uottawa.ca*

Abstract: Brillouin grating in optical fibers is of considerable interest due to its applications in optical fiber communication and distributed sensing. However, the intrinsic Brillouin grating spectrum is still unknown and several kinds of spectra were reported. In this paper, we experimentally investigate the characteristics of the Brillouin grating spectra in a polarization-maintaining fiber, and the results show that it agrees with the theory of fiber Bragg grating but not determined by the natural Brillouin gain bandwidth as thought previously, and in the case of weak grating, the bandwidth is only length-limited, i.e., inversely proportional to the length of the Brillouin grating. In addition, the apodization of the Brillouin grating induced by the acoustic wave decay, a unique feature that is different from the Bragg grating, is observed for the first time to the best of our knowledge.

OCIS codes: (290.5900) Scattering, stimulated Brillouin; (060.3735) Fiber Bragg gratings; (190.4370) Nonlinear optics, fibers.

References and links

1. Z. Zhu, D. J. Gauthier, and R. W. Boyd, "Stored light in an optical fiber via stimulated Brillouin scattering," Science **318**(5857), 1748–1750 (2007).
2. Y. Cao, P. Lu, Z. Yang, and W. Chen, "An efficient method of all-optical buffering with ultra-small core photonic crystal fibers," Opt. Express **16**(18), 14142–14150 (2008).
3. V. P. Kalosha, W. Li, F. Wang, L. Chen, and X. Bao, "Frequency-shifted light storage via stimulated Brillouin scattering in optical fibers," Opt. Lett. **33**(23), 2848–2850 (2008).
4. W. Zou, Z. He, and K. Hotate, "Complete discrimination of strain and temperature using Brillouin frequency shift and birefringence in a polarization-maintaining fiber," Opt. Express **17**(3), 1248–1255 (2009).
5. W. Zou, Z. He, K. Y. Song, and K. Hotate, "Correlation-based distributed measurement of a dynamic grating spectrum generated in stimulated Brillouin scattering in a polarization-maintaining optical fiber," Opt. Lett. **34**(7), 1126–1128 (2009).
6. Y. Dong, X. Bao, and L. Chen, "Distributed temperature sensing based on birefringence effect on transient Brillouin grating in a polarization-maintaining photonic crystal fiber," Opt. Lett. **34**(17), 2590–2592 (2009).
7. K. Y. Song, and H. J. Yoon, "High-resolution Brillouin optical time domain analysis based on Brillouin dynamic grating," Opt. Lett. **35**(1), 52–54 (2010).
8. K. Y. Song, W. Zou, Z. He, and K. Hotate, "Optical time-domain measurement of Brillouin dynamic grating spectrum in a polarization-maintaining fiber," Opt. Lett. **34**(9), 1381–1383 (2009).
9. W. Zou, Z. He, and K. Hotate, "Demonstration of Brillouin distributed discrimination of strain and temperature using polarization-maintaining optical fiber," IEEE Photon. Technol. Lett. **22**(8), 526–528 (2010).
10. K. Y. Song, K. Lee, and S. B. Lee, "Tunable optical delays based on Brillouin dynamic grating in optical fibers," Opt. Express **17**(12), 10344–10349 (2009).
11. Y. Dong, L. Chen, and X. Bao, "Truly distributed birefringence measurement of polarization-maintaining fibers based on transient Brillouin grating," Opt. Lett. **35**(2), 193–195 (2010).
12. K. Y. Song, W. Zou, Z. He, and K. Hotate, "All-optical dynamic grating generation based on Brillouin scattering in polarization-maintaining fiber," Opt. Lett. **33**(9), 926–928 (2008).
13. A. A. Fotiadi, R. V. Kiyan, and E. A. Kuzin, "SBS induced hypersound dynamic grating in multimode optical fibers: Phase conjugation specific features," *in Proceedings of IEEE Conference on Laser and Electro-Optics society Annual Meeting* (IEEE, 1997), pp. 44–45.
14. T. Erdogan, "Fiber grating spectra," J. Lightwave Technol. **15**(8), 1277–1294 (1997).
15. R. W. Boyd, *Nonlinear Optics*, (Academic Press) 3rd edition, Chap. 9.
16. A. Melloni, M. Frasca, A. Garavaglia, A. Tonini, and M. Martinelli, "Direct measurement of electrostriction in optical fibers," Opt. Lett. **23**(9), 691–693 (1998).

#130150 - $15.00 USD Received 15 Jun 2010; revised 15 Jul 2010; accepted 12 Aug 2010; published 20 Aug 2010

17. A. A. Fotiadi, R. Kiyan, O. Deparis, P. Mégret, and M. Blondel, "Statistical properties of stimulated Brillouin scattering in single-mode optical fibers above threshold," Opt. Lett. **27**(2), 83–85 (2002).

1. Introduction

There is an increasing interest over recent years in Brillouin grating (also called transient Brillouin grating or Brillouin dynamic grating) in optical fibers due to its applications in optical storage [1–3], distributed sensing [4–9], optical delay line [10], and birefringence characterization of polarization-maintaining fiber (PMF) [11]. Generally, a Brillouin grating is generated by using two counter-propagating pump waves through stimulated Brillouin scattering (SBS) [12,13]. A Brillouin grating in fact is a moving periodically modulated refractive index associated with an acoustic wave, which results from the interaction between two pump waves through electrostriction effect. Compared with conventional fiber Bragg gratings, the Brillouin gratings have two unique features: one is that it is a moving grating, which can produce a Brillouin frequency shift (BFS) to the reflected light with respect to the probe wave, and the other is that there is a lifetime (~10 ns for silica fiber) for its existence after removing the pump waves [11]. For most applications, a high-birefringence PMF is used, where two pump waves are launched into one axis of the PMF to create a Brillouin grating and a probe wave is launched into the other axis to read the grating. A maximum reflection on the Brillouin grating can be seen when the frequency difference between the probe wave and the pump wave, who propagates in the same direction as the probe wave, satisfies the phase matching condition, i.e. $\Delta\nu_{Bire} = \Delta n\nu/n_g$, where Δn is the phase birefringence of the PMF, n_g is the group refractive index, and ν is the frequency of probe wave [11,12].

A Brillouin grating can be generated in correlation domain [4,5,9] and time domain [6–8,10–12], respectively. In the correlation-based technique, a Brillouin grating is generated using two synchronized and frequency-modulated CW pump waves. In time domain, a Brillouin grating can be more conveniently generated through two frequency-locked pump waves, which includes three schemes in terms of pump type. The first scheme uses two CW pumps, and the Brillouin grating can exist in the whole fiber [4,12]. However, due to the nonuniformities of BFS and the birefringence of PMF [11], the measured Brillouin grating spectra can be broadened inhomogeneously [4,8]. The second scheme includes a CW pump and a pump pulse, where the Brillouin grating is generated following the pump pulse from one end to the other end [7,8]. In this case, due to the decay of the acoustic wave, the length of the existing Brillouin grating is limited to $L_B = (t_P + \tau_B)c/n$, where t_P is the width of pump pulse, τ_B is the phonon lifetime and n is the fiber refractive index. The third scheme includes two short pump pulses (< 10 ns), where the Brillouin grating can be generated at a specific location controlled by the delay of the two pump pulses [6,11]. The interaction length of the two pulses is $L = (t_{P1} + t_{P2})c/2n$, where t_{P1} and t_{P2} are the pulse widths of pump 1 and pump 2, respectively. However, due to the phonon excitation time, the effective length of Brillouin grating is only half of the interaction length, i. e. $L_B = (t_{P1} + t_{P2})c/4n$, for example, 20 cm for two 2 ns pump pulses [6,11].

Up to now, several kinds of spectra were obtained in experiment and the intrinsic Brillouin grating spectrum is still unknown. In Ref. 12, an asymmetric spectrum with a FWHM (full width at the half maximum) of 80 MHz was obtained. In Ref. 8, the measured spectra show asymmetry and some irregular side lobes, and the FWHM ranges from 50 MHz to 100 MHz. In Ref. 4, a symmetric Gaussian-like spectrum with a FWHM of ~320 MHz was obtained. In Ref. 11, the measured spectra show a two-peak structure. In Ref. 10, the Brillouin grating spectrum was thought to have a relationship with the natural Brillouin gain bandwidth. In this paper, we experimentally investigate the intrinsic Brillouin grating spectra with two pump pulses, where a short Brillouin grating can be obtained to avoid the impact on spectrum induced by nonuniform birefringence of PMF. The length of the Brillouin grating can be

#130150 - $15.00 USD Received 15 Jun 2010; revised 15 Jul 2010; accepted 12 Aug 2010; published 20 Aug 2010

precisely controlled through changing the pump pulse width. The measured results show that the Brillouin grating spectra agree with the theory of fiber Bragg grating, and in the case of weak grating (very small refractive index change), the bandwidth is only length-limited, i.e., inversely proportional to the length of the Brillouin grating. In addition, the apodization of the Brillouin grating induced by acoustic wave decay, a unique feature that is different from the Bragg grating, is observed for the first time to the best of our knowledge.

2. The criteria of weak Brillouin grating

The perturbation of refractive index associated with an acoustic wave can be expressed by

$$\delta n = \overline{\delta n}\left[1 + v\cos\left(\Omega_{\mathrm{B}} t \pm \frac{2\pi}{\Lambda} z\right)\right] \tag{1}$$

where $\overline{\delta n}$ is the average index change over a grating period, v is the fringe visibility of the index change, Ω_{B} is the Brillouin frequency, $\Lambda = \lambda/2n$ is the grating period, and λ is the vacuum wavelength of pump wave, n is the fiber refractive index. This equation is similar as that of fiber Bragg grating except the term $\cos\left(\Omega_{\mathrm{B}} t \pm 2\pi z/\Lambda\right)$ [14], which indicates that it is a moving grating.

SBS is a resonant electrostriction effect in a material that is compressed in presence of an electric field. We represent the change in the susceptibility in the presence of an optical field as $\Delta\chi = \Delta\varepsilon$. Ignoring the DC term, the AC modification of the optical properties of a material system induced by SBS is given by [15]

$$\Delta\chi = \varepsilon_0 C_T \gamma_e^2 E_P E_S \tag{2}$$

where $\varepsilon_0 = 8.85\times10^{-12}\ F/m$ is the vacuum permittivity, C_T is the compressibility, γ_e is the electrostriction constant. Using $\Delta\varepsilon \cong 2n\delta n$, we have

$$v\overline{\delta n} = \frac{\varepsilon_0 C_T \gamma_e^2 E_P E_S}{2n} \tag{3}$$

where E_P and E_S are electric fields of pump and Stokes waves, respectively.

For a weak fiber Bragg grating, whose $v\overline{\delta n}$ is very small, its bandwidth is only determined by the length of the grating, also said to be "length-limited", and can be simply given by [14]

$$\Delta\nu = \frac{c}{2nL};\quad \left(v\overline{\delta n} \ll \frac{\lambda}{L}\right) \tag{4}$$

here $\Delta\nu$ is the FWHM bandwidth, L is the length of the grating. In our case, the generated Brillouin gratings are all shorter than 1 m because of using short pump pulses. The criteria of the weak Brillouin grating with a length of 1 m at wavelength of 1.55 μm is $v\overline{\delta n} \ll 1.55\times10^{-6}$.

In our experiment, the peak power of two pump pulses acting as pump wave and Stokes wave are 0.4 W and 30 W, and the corresponding electric fields in a single-mode fiber are roughly 4×10^6 V/m and 3×10^8 V/m, respectively. In a silica optical fiber there are $C_T = 2.71\times10^{-11}\mathrm{m}^2/\mathrm{N}$, $\gamma_e = 0.902$ and $n = 1.45$ [16]. Using Eq. (3), we have $v\overline{\delta n} = 8.1\times10^{-8}$, which satisfies the criteria of the weak Brillouin grating. Note that Eq. (3) is for steady SBS process, for which the pump and Stokes pulse widths should be both longer

#130150 - $15.00 USD Received 15 Jun 2010; revised 15 Jul 2010; accepted 12 Aug 2010; published 20 Aug 2010

than τ_B, so that the induced $v\overline{\delta n}$ could be even smaller for transient SBS process with pump or Stokes pulse shorter than τ_B.

3. Principle and experimental setup

In our scheme, illustrated in Fig. 1, a Brillouin grating is generated by two pump pulses. The frequency of pump 1 is higher than that of pump 2 by a Ω_B of optical fiber, and the Brillouin grating has the same motion direction as pump 1. The effective length of the Brillouin grating is $L_B = (t_{P1} + t_{P2})c/4n$. In experiment, t_{P2} is fixed at 2 ns and t_{P1} is increased from 2 ns to 6 ns to increase the effective length of the Brillouin grating from 0.2 m to 0.4 m. Two pump pulses are launched into the slow axis of PMF, and the probe pulse immediately following pump 2 pulse (the leading edge of probe pulse overlapping with trailing edge of pump 2 pulse) is launched into the fast axis to read the Brillouin grating. Because the probe pulse counter-propagates with the Brillouin grating, coherent anti-Stokes Brillouin scattering (CABS) could occur when the probe pulse interacts with the Brillouin grating, and consequently the scattered light frequency is higher than that of probe pulse by a Ω_B. The CABS will be maximized when the frequency difference $\Delta\nu_{Bire}$ between pump 2 and the probe satisfies the phase-matching condition [11,12].

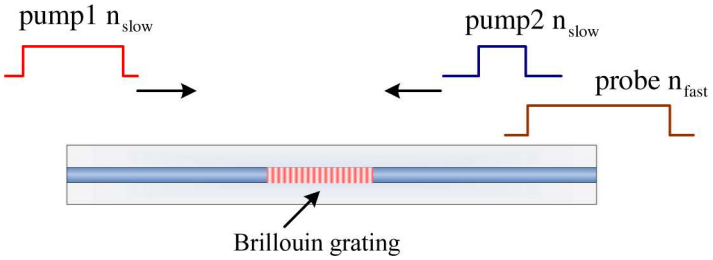

Fig. 1. Schematic diagram of Brillouin grating generation and reading.

The experimental setup is shown in Fig. 2. Two narrow linewidth (3 kHz) fiber lasers operating at 1550 nm are used to provide the pump1 and pump2, respectively, and their frequency difference is locked by a frequency counter. A tunable laser with a wavelength resolution of 0.1 pm is used as probe wave. The frequency difference between pump1 and probe is monitored and recorded by a high-speed detector with a bandwidth of 45 GHz and a 44 GHz electrical spectrum analyzer. Three high extinction-ratio (ER) electro-optic modulators (> 45 dB) are used to generate pump 1, pump 2 and probe pulses. The power of pump 1 pulse, pump 2 pulse and probe pulse in the PMF are about 0.4W, 30 W and 30 W, respectively. A tunable fiber Bragg grating with a bandwidth of 0.2 nm is used to filter out the transmitted pump1 pulse.

A Panda fiber is used in experiment, whose nominal beat-length is smaller than 5 mm at 1550 nm with a BFS of 10.871 GHz at room temperature.

#130150 - $15.00 USD Received 15 Jun 2010; revised 15 Jul 2010; accepted 12 Aug 2010; published 20 Aug 2010

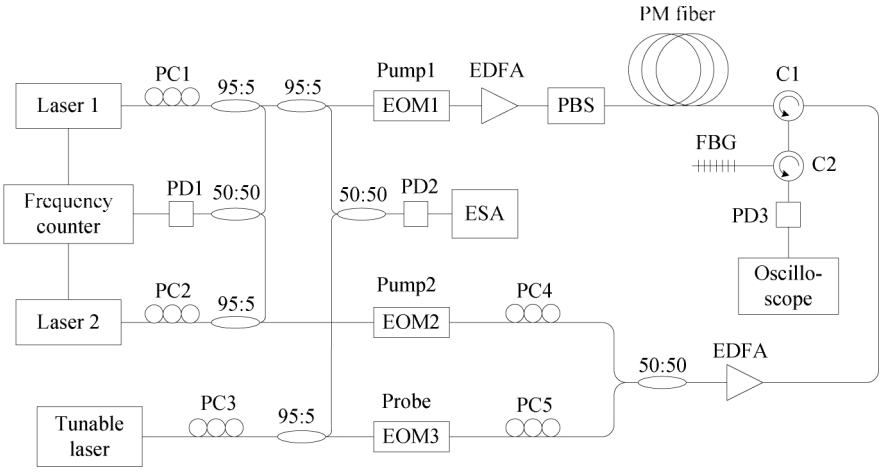

Fig. 2. Experimental setup. PC: polarization controller, EOM: electro-optic modulator, PBS: polarization beam splitter, C: circulator, PD: photo-detector, EDFA: Erbium-doped fiber amplifier, ESA: electrical spectrum analyzer, FBG: fiber Bragg grating.

4. Results and discussions

In Ref. 11, a two-peak structure Brillouin grating spectra were obtained, which was mistakenly explained to be the fine structure of the optical mode. In this paper, we found that the two-peak spectra were induced by the leakage of pump 1 pulse. In experiment, the pump 1, pump 2 and probe pulses were set to 2 ns, 2 ns and 6 ns, respectively. The comparison of measured Brillouin grating spectra with different ER of pump 1 pulse is shown in Fig. 3. The leakage of pump 1 pulse decreases the power of the reflected probe pulse especially when the frequency offset between the probe wave and the pump wave satisfies the phase matching condition, which decreases the intensity of the spectrum and causes a dip at the center of the spectrum resulting in a two-peak structure. The impact of the leakage can be removed by using high ER modulators, and a one-peak spectrum can be obtained as shown in Fig. 3.

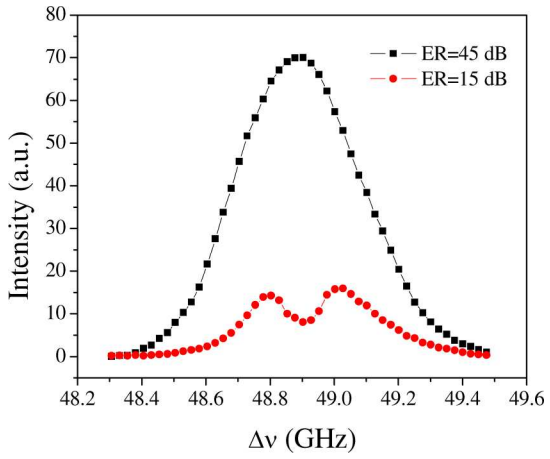

Fig. 3. Measured Brillouin grating spectra with different ER (45 dB and 15 dB) of pump 1 pulse.

Then we investigated the Brillouin grating spectra with different grating lengths. t_{P2} was fixed at 2 ns and t_{P1} was increased from 2 ns to 6 ns to increase the effective length of the Brillouin grating from 0.2 m to 0.4 m. The probe pulse width of 6 ns and 8 ns were chosen to read the Brillouin grating, and the measured Brillouin grating spectra are shown in Fig. 4. For

#130150 - $15.00 USD Received 15 Jun 2010; revised 15 Jul 2010; accepted 12 Aug 2010; published 20 Aug 2010

the case of 2 ns pump 1 pulse and 2 ns pump 2 pulse, the effective length of the generated Brillouin grating is 0.2 m and the measured spectra are shown in Fig. 4(a), which fit well with a Gaussian profile. The intensity of the acoustic wave is determined by the interaction time of the pump and the Stokes waves, and thus the generated Brillouin grating is a nonuniform-grating with δn maximizing at the center and decreasing toward two sides. This nonuniform apodization of Brillouin grating results in a Gaussian spectrum without side lobes, which are expected in a uniform-grating [14].

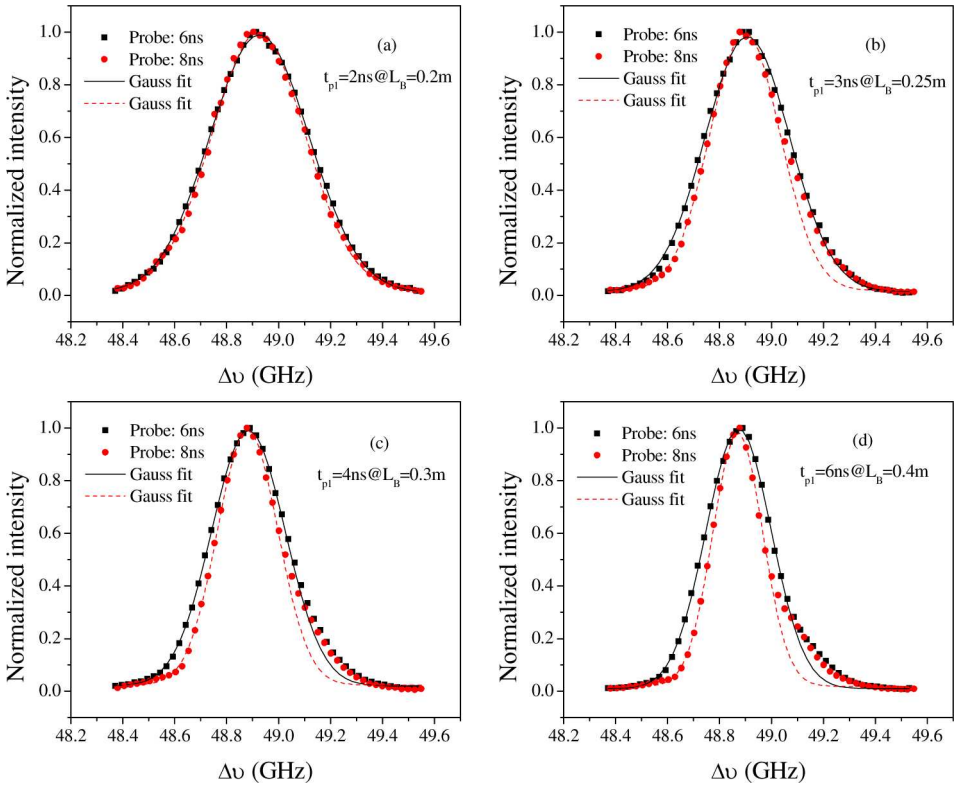

Fig. 4. Measured Brillouin grating spectra with 6 ns and 8 ns probe pulse with different pump 1 pulse width (a) 2 ns, (b) 3 ns, (c) 4 ns, (d) 6 ns. Pump 2 pulse width is constant at 2 ns.

The measured spectrum is the convolution of the probe pulse spectrum and the intrinsic Brillouin grating spectrum, which has been pointed out in previous works [6,17]. The intrinsic Brillouin grating spectrum can be obtained from deconvoluting the probe pulse spectrum out of the measured spectra, and the spectral widths (FWHM) are plotted in Fig. 5. The black curve shows the FWHM spectrum width of weak fiber Bragg grating described by Eq. (4). For 8 ns probe pulse, the measured spectral widths agree very well with the theory of weak fiber Bragg grating; for 6 ns probe pulse, the experimental results also agree with the theoretical curve when the grating length is shorter than 0.3 m, while the discrepancy from the theory at 0.4 m originates from the effective reading-length of the 6 ns probe pulses. These results directly prove that the moving Brillouin grating and the static fiber Bragg grating follow the same basic theory.

#130150 - $15.00 USD Received 15 Jun 2010; revised 15 Jul 2010; accepted 12 Aug 2010; published 20 Aug 2010

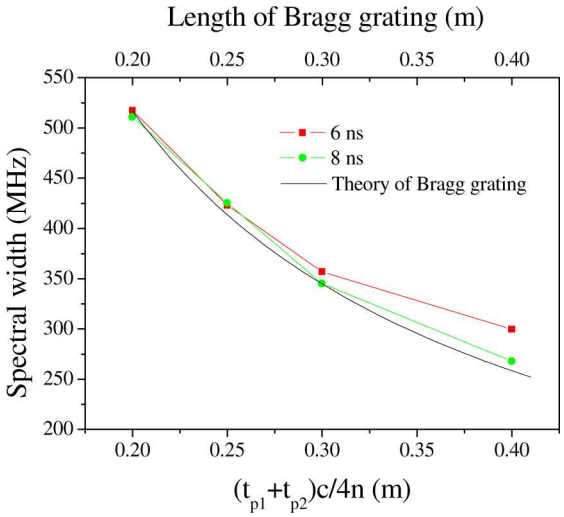

Fig. 5. The intrinsic Brillouin grating spectral width as a function of length.

The other important characteristic of the Brillouin grating is the acoustic wave relaxation or grating decay. The Brillouin grating is created through electrostriction effect and can only be sustained by keeping the two pump waves. After removing the pump waves, the Brillouin grating will exponentially decay, which characterizes an intrinsic Lorentzian Brillouin gain spectrum [15]. In our scheme as shown in Fig. 1, pump 2 pulse is fixed at 2 ns and pump 1 pulse width is increased to prolong the grating length. The Brillouin grating is generated following pump 2 pulse from the right end to the left end, and the intensity of the whole Brillouin grating exhibit a slope due to the acoustic wave decay. For the probe pulse immediately following pump 2 pulse, the front of the probe pulse always read the strongest part of the grating, while the rear of the probe pulse always read the decayed part, which causes the asymmetry of the spectra especially for long gratings as shown in Fig. 4. It is clearly seen that for long gratings the low-frequency side still agrees well with Gaussian profile, while the high-frequency side has a discrepancy and shows a Lorentzian-like wing, which comes from the apodization of the Brillouin grating induced by acoustic wave decay.

To further demonstrate the effect of the apodization of the Brillouin grating induced by the acoustic wave decay, we switched the pulse width of pump 1 and pump 2 pulses with probe pulse still immediately following pump 2 pulse. Figure 6 shows the measured Brillouin grating spectrum with 2 ns pump 1 pulse, 10 ns pump 2 pulse and 6 ns probe pulse. In this case, the Brillouin grating is created following pump 1 pulse from the left end to the right end, and both of the front and the rear of the probe pulse read the decayed grating. We see that the measured spectrum agrees with a Lorentzian profile, which indicates that the acoustic wave decay play an important role in this case. For the case of 2 ns pump 1 and 2 ns pump 2, it is a transient process, where the interaction duration is much smaller than the phonon lifetime, and consequently the grating decay can be neglected, so that the spectra have a Gaussian profile as shown in Fig. 4(a).

#130150 - $15.00 USD Received 15 Jun 2010; revised 15 Jul 2010; accepted 12 Aug 2010; published 20 Aug 2010

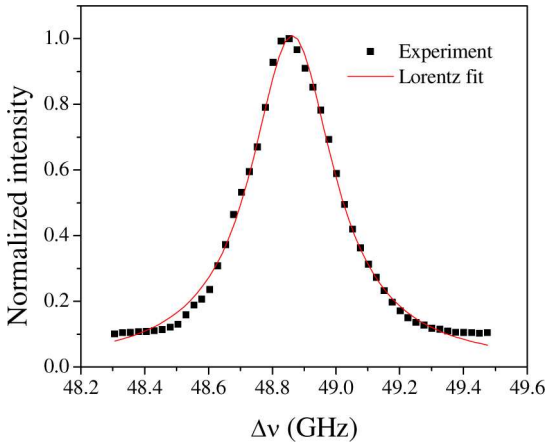

Fig. 6. Measured Brillouin grating spectrum with 2 ns pump 1 pulse, 10 ns pump 2 pulse and 6 ns probe pulse.

In addition, pump depletion can also cause Brillouin grating apodization. In our case, pump 1 and pump 2 correspond to the pump wave and Stokes wave in the SBS process. Because of short interaction duration (2 ns), only a small fraction of power is transferred from pump 1 to pump 2, so that the pump depletion can be negligible when a Brillouin grating is generated.

5. Conclusion

In summary, we have investigated the characteristics of the Brillouin grating spectra. First, the criteria of the weak Brillouin grating is analyzed and the calculations show that the Brillouin grating generated in our experiment are in the regime of weak grating. Then we experimentally demonstrated that the Brillouin grating spectrum agrees with the fiber Bragg grating theory but not determined by the natural Brillouin gain bandwidth as thought previously. The apodization of the Brillouin grating induced by the acoustic wave decay were also observed, and both Gaussian and Lorentzian spectra can be obtained depending on the effect of acoustic wave decay. Compared with the fixed fiber Bragg grating, the Brillouin grating can be conveniently created at arbitrary position with variable length, which can be used as a position- and bandwidth-adjustable filter in sensing, optical communication and other applications.

Acknowledgments

The authors would like to thank Natural Science and Engineering Research Council of Canada (NSERC) Discovery Grants and Canada Research Chair program for the financial support of this research.

#130150 - $15.00 USD Received 15 Jun 2010; revised 15 Jul 2010; accepted 12 Aug 2010; published 20 Aug 2010